Catalysis Today 154 (2010) 224–228

Contents lists available at ScienceDirect

Catalysis Today

journal homepage: www.elsevier.com/locate/cattod

Irreversible deactivation of styrene catalyst due to potassium loss—Development of antidote via mechanism pinning

Weronika Bieniasz*, Michał Trębala, Zbigniew Sojka, Andrzej Kotarba*

Faculty of Chemistry, Jagiellonian University, Ingardena 3, 30-060 Krakow, Poland

ARTICLE INFO

Article history:
Available online 24 April 2010

Keywords:
Styrene catalyst
Potassium ferrites
$K_2Fe_{22}O_{34}$
Potassium loss
Stability
Iron oxides
Work function

ABSTRACT

Potassium loss processes involved in irreversible deactivation of the β-ferrite component of the styrene catalyst were investigated by means of Species Resolved Thermal Alkali Desorption and work function measurements in the process temperature range. Two main mechanisms of the stabilization were developed depending on the dopant location. It was found that incorporation of Cr promoter into the structure of β-ferrite slows down potassium diffusion from the bulk towards the surface, whereas the additive segregated at the basal planes (such as CeO_2), favoring the cationic state of potassium, inhibits the probability of potassium atoms to leave the $K_2Fe_{22}O_{34}$ surface via work function increase. From the obtained results it may be concluded that K loss can be effectively extinguished via appropriate doping of the less stable β-ferrite active phase of the iron-oxide catalyst.

1. Introduction

Ethylbenzene dehydrogenation is the major catalytic dehydrogenation process carried out in petrochemical industry. The worldwide annual production of styrene monomer exceeds 2×10^7 ton and makes it after ethylene, vinyl chloride and propylene one of the most used monomers [1]. The most widespread production route of styrene is the catalytic ethylbenzene dehydrogenation. The commercial process is carried out in adiabatic or isothermal mode in fixed bed reactor with radial or axial flow of the reactants. The process is highly endothermic ($\Delta H_{873K} = 124.9\,kJmol^{-1}$) and is accompanied with an increase in moles of the reactants. Most styrene production units are operated under atmospheric or reduced pressure in temperature range of 550–650 °C and the typical water-to-ethylbenzene ratio of 12:1 depending slightly on the catalyst and process used [2].

The commercial catalyst for the most styrene plants is based on iron oxide promoted with potassium with small amount of several additives—usually Al [3], Ce [4,5], Cr [6], Mg [7], Mn [8], Mo [9], Ti [10], and Zn [11].

Whereas, potassium acts as a chemical promoter increasing the catalyst activity by an order of magnitude, the other additives are textural and surface modifiers, stabilizing the high specific surface area of the catalyst.

The main reasons for the iron-oxide catalyst deactivation in severe industrial conditions include formation of carbonaceous deposit, and loss of potassium promoter. While the first factor is reversible, and coke removal is achieved by steam co-feeding, the second factor is irreversible, and leads to the activity decay during the time on stream operation. Thus the comprehensive research has been dedicated to potassium loss processes from the model and real iron-oxide catalysts [12,13].

The interaction of potassium with iron-oxide matrix leads to a multicomponent, multiphase system with the following phases reported in open literature and patents: α- and γ-Fe_2O_3, Fe_3O_4, KOH, K_2CO_3, $KFeO_2$ and $K_2Fe_{22}O_{34}$ [5,14]. The iron-oxide catalyst precursor corresponds to K-doped hematite. In the course of the solid-state restructuring two ferrite phases, $KFeO_2$ and $K_2Fe_{22}O_{34}$, are formed and the active state of the catalyst surface is assigned to the equilibrium between them. The potassium thermal desorption studies revealed that the $K_2Fe_{22}O_{34}$ β-ferrite, due to its specific layered β-alumina structure is principally responsible for potassium volatilization from the styrene catalyst [15]. Additionally, it was shown that introduction of alien metal ions can substantially improve the stability of $K_2Fe_{22}O_{34}$, whereas in the case of $KFeO_2$ the reverse effect of pronounced potassium thermal destabilization was observed [16].

Although potassium ferrites make the real iron-oxide catalyst active and selective, the severe process conditions accelerate its steady deterioration due to potassium loss and redistribution, requiring regular replacement of the catalyst in the installation every 1–2 years. A concise review of these problems can be found elsewhere [12]. Consequently, the investigations of potassium loss mechanism, as well as understanding of the influence of the addi-

* Corresponding authors. Tel.: +48 12 663 20 17; fax: +48 12 634 05 15.
E-mail addresses: rozek@chemia.uj.edu.pl (W. Bieniasz), kotarba@chemia.uj.edu.pl (A. Kotarba).

0920-5861/$ – see front matter © 2010 Elsevier B.V. All rights reserved.
doi:10.1016/j.cattod.2010.03.059

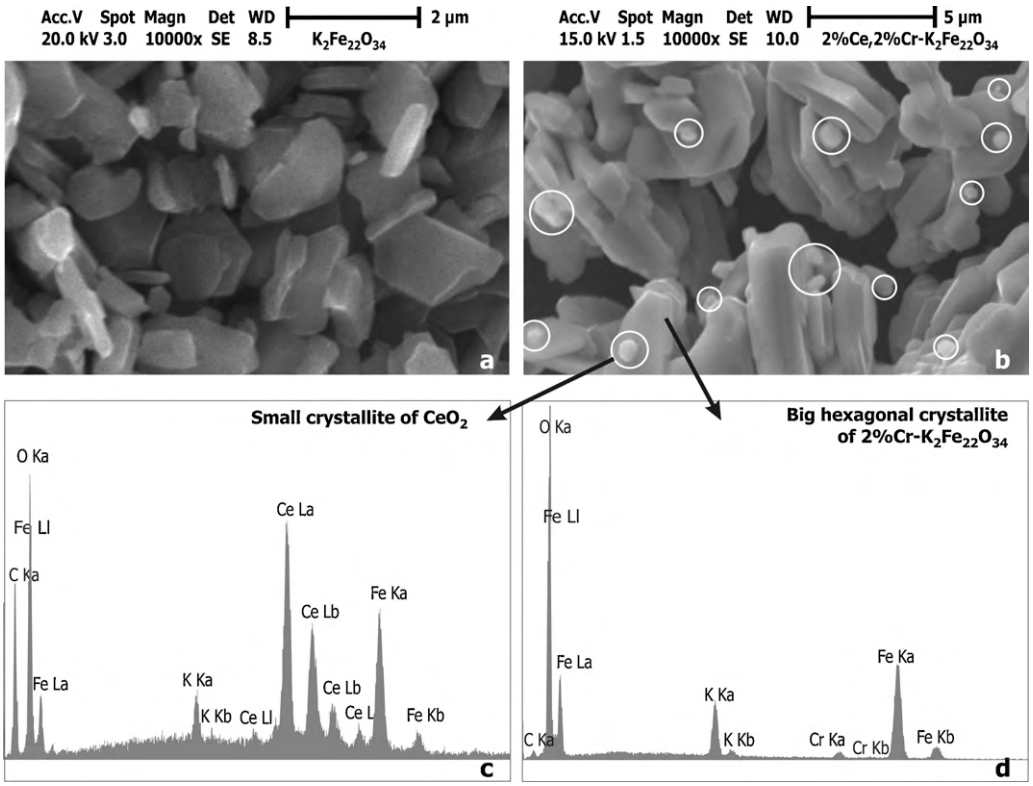

Fig. 1. SEM images of undoped (a) and 2% Cr + 2% Ce-doped (b) $K_2Fe_{22}O_{34}$ together with the EDX spectra (c and d) showing different localization of the dopants. Whereas chromium was incorporated into the hexagonal plates of $K_2Fe_{22}O_{34}$, cerium in the form of round shape crystallites of CeO_2 (encircled) segregated at the β-ferrite basal planes.

tives on these processes in the β-ferrite – the principal phase associated with the catalyst activity – are required.

The aim of the study was to investigate potassium migration, segregation and desorption processes involved in irreversible deactivation of the β-ferrite component of the styrene catalyst, and to develop an effective antidote based on mechanistic understanding. The potassium loss process was investigated by means of Species Resolved Thermal Alkali Desorption in tandem with a transient Field Reversal studies in the process temperature range corroborated by the work function measurements.

2. Experimental

Series of pristine, mono- and double-promoted phase of $K_2Fe_{22}O_{34}$ was prepared by the ceramic synthesis of K_2CO_3 and α-Fe_2O_3. The procedure was described previously elsewhere [17]. To obtain $K_2Fe_{22}O_{34}$, stoichiometric amounts of substrates were finely grounded for 30 min in an agate mortar. The mixture in a porcelain crucible was placed in a box-type furnace, heated up to 900 °C with a heating rate of 7.5 °C/min, kept in that temperature for 1 h, and cooled down to the room temperature. The sintered powder was next regrounded for 15 min and calcined again at 1200 °C for 5 h. For doped samples 0.1–5 wt.% of α-Fe_2O_3 was replaced by Cr_2O_3, CeO_2, MgO, Al_2O_3, MnO_2. This level of doping was chosen as a typical range applied in industrial practice as described in the open and patent literature.

The BET-N_2 surface area of the samples was determined with the use of Quantasorb apparatus. All the investigated samples exhibited alike surface area of $5 \pm 2\ m^2/g$, within the experimental limit.

The phase composition of the synthesized materials was examined by X-ray diffraction. The measurements were performed with CuKα radiation in the Bragg-Brentano geometry using X'pert Pro Philips powder diffractometer. The morphology of the samples was examined with a Philips scanning electron microscope model XL 30 ESEM at magnifications of ×10,000.

The kinetic parameters of potassium desorption and diffusion (activation energies, rate constants, flux intensities) were determined by Species Resolved Thermal Alkali Desorption [15] and Field Reversal [18] methods in the process temperature range (500–650 °C). The experiments were carried out in a vacuum chamber under the pressure of 10^{-8} mbar. The samples, formed into the wafers of 10-mm diameter and mass of 100 mg, were heated from room temperature to 650 °C in the stepwise mode at the rate of 5 °C/min, waiting after each temperature ramp for steady-state signal. For each temperature the resultant positive current was averaged over ten independent data points and measured with the use of Keithley 6512 digital electrometer.

Due to the low ionization potential of potassium ($I = 4.3$ eV) from solid surfaces potassium is thermally emitted in the form of atoms and ions [13,15,16]. In the case of steady-state measurements, the samples were biased with a positive potential of +60 V to accelerate the K^+ ions towards the collector. Since the Arrhenius-type plots (logarithms of measured K and K^+ signals versus T^{-1}) for potassium ions and atoms are linear (correlation coefficients better than 0.995), the corresponding activation energies of the desorption could be reliably determined, as shown in [15,16].

The field reversal method has been discussed in detail previously [18]. The basic idea of the method is to periodically block the potassium ionic desorption channel by changing the surface potential. When the ionic desorption channel is blocked by a retarding field, only neutral potassium desorption influences the surface concentration of the alkali promoter, which increases to a new and higher steady-state value. When the retarding field is switched again to an accelerating one, the ionic channel is opened and the surface concentration of potassium decreases towards the original steady-state value. In the present field reversal experiments the samples were kept at the constant temperature in the range of 550–650 °C.

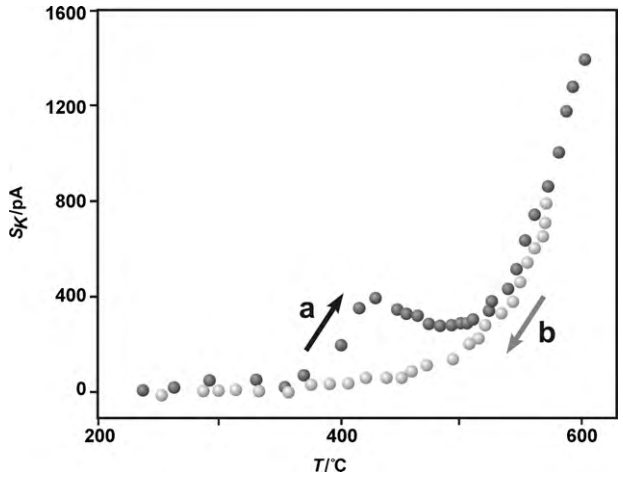

Fig. 2. Typical changes in potassium desorption signal as a function of temperature for Cr-doped β-ferrite with the increasing (a) and decreasing (b) temperature ramp.

A switching circuit give rise and fall times in the order of 1 ms between 0 and +75 V applied to the sample during the experiments. A Faraday cup detector was placed at a distance of 90 mm from the investigated surface, and was used to detect the transient signal due to emitted K^+ ions. The transient signal was amplified and acquired by a 250 MHz digital oscilloscope (Instek GDS-8405).

The changes in the surface work function were carried out under the vacuum of 10^{-7} mbar with the use of the samples pressed into the pellets (diameter 10 mm, 5 MPa). The contact potential difference (V_{CPD}) measurements were carried out by the dynamic condenser method of Kelvin with a KP6500 probe (McAllister Technical Services) at 550 °C. The reference electrode was a standard stainless steel plate with diameter of 3 mm (Φ_{ref} = 4.3 eV) provided by the manufacturer. During the measurements the gradient of the peak-to-peak versus backing potential was set to 0.2, whereas the vibration frequency and amplitude were set to 120 Hz and 40 a.u. The final V_{CPD} value was an average of 50 independently measured points. The changes in the V_{CPD}, equivalent to changes in the surface work function ($\Delta\Phi$) were monitored for about 3 h.

3. Results and discussion

The diffraction patterns of the synthesized undoped and doped $K_2Fe_{22}O_{34}$ ferrites showed that the samples were monophasic until the level of doping exceeded 5 wt.%, and were consistent with the

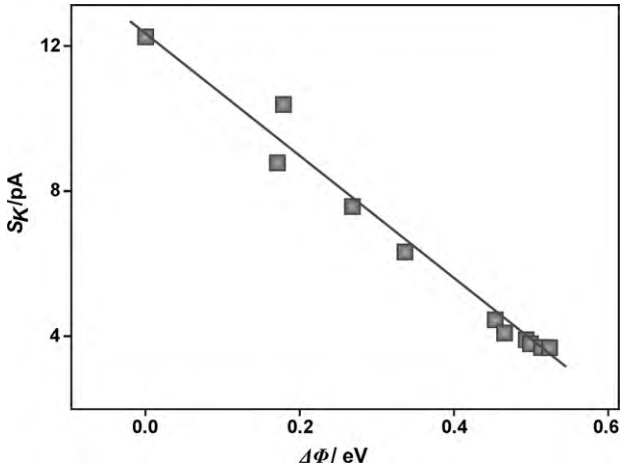

Fig. 3. The linear correlation between the potassium desorption flux and the work function of the β-ferrite sample.

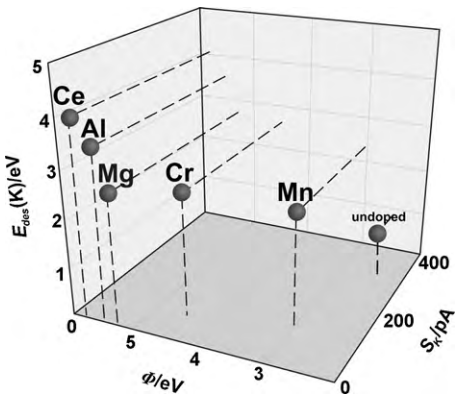

Fig. 4. 3D diagram: desorption energies of potassium atoms (E_{des}), work function (Φ) and potassium desorption signal (S_K) used for evaluation of the effect of dopants on stability of the β-ferrite.

*P*63/*mmc* (JCPDS-ICDD 31-1034) space group. The introduction of chromium and cerium into the $K_2Fe_{22}O_{34}$ does not influence its structure in an appreciable way [16]. The well-developed plate crystallites of hexagonal shape (~2 μm in diameter and thickness of 0.2–0.3 μm) are characteristic for β-$K_2Fe_{22}O_{34}$ crystals with stoichiometric composition [17,19]. In general, the size and shape of crystallites were found to be very similar for undoped and doped β-$K_2Fe_{22}O_{34}$ as shown in Fig. 1. However, the closer inspection of the Ce-doped samples reveals that the large plate-like β-ferrite crystallites are decorated by smaller round isometric crystallites of ~0.1 μm in diameter (a few of them are marked with white circles in Fig. 1b for better perception). The EDX elementary analysis performed for several grains gave essentially the same picture and confirmed that the plate-like crystallites contained only the constituent elements of β-ferrite and also showed that chromium is incorporated in the bulk of the ferrite crystallites. The small round crystallites located at the basal hexagonal planes were identified as CeO_2 (Fig. 1d), which revealed that this dopant is completely segregated at the β-ferrite surface.

There are two main reasons why potassium is commonly used as a promoter in the iron-oxide catalyst: formation of active phases and limitation of the building up of the carbonaceous deposits by promoting gasification reaction. Thus, it is necessary that the potassium containing compounds have to be available at the working catalyst surface. This in turn, taking into account relatively high temperature of the styrene production process, leads to unavoidable progression of potassium loss. In general, during the potassium loss from the iron-oxide catalyst migration, segregation and desorption processes are involved [12,13].

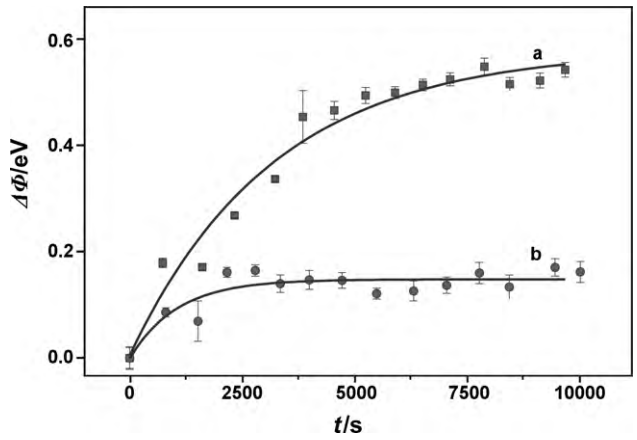

Fig. 5. Changes in the work function versus time for undoped (a) and 2% Cr-doped β-ferrite (b) measured at the temperature of 550 °C.

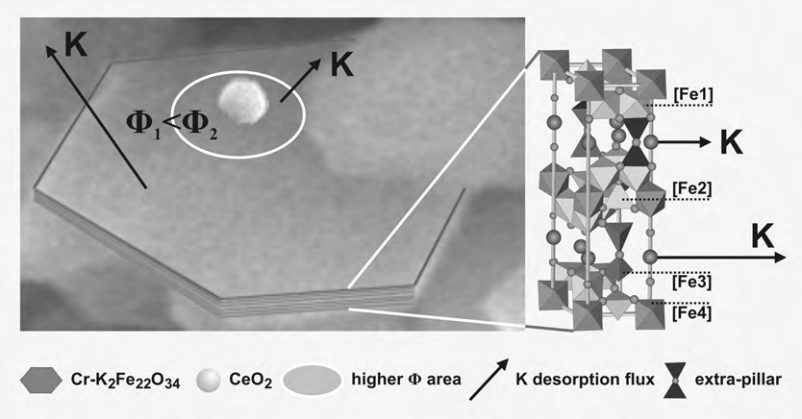

Fig. 6. The conceptual model showing two mechanisms of potassium stabilization in β-ferrite via surface (CeO_2) and structural (Cr^{3+}) doping. The white ellipse indicates the presumable area of enhance work function induced by ceria.

Although the desorption fluxes of K^+ ions, K^* excited states, K_n clusters and KOH were also reported [13] for the iron-oxide catalyst, they are of secondary importance in the total potassium loss volatilization balance, which is dominated by the atomic flux [16]. The typical profile of the K desorption flux from the surface measured with increasing and decreasing temperature is shown in Fig. 2. The inspection of the figure revealed that the onset of the appreciable K desorption is observed at the temperature below 400 °C. When the sample was heated up the K signal exhibited a characteristic local maximum in the low temperature range (Fig. 2a). The monotonous exponential change of the potassium desorption signal (S_K) with temperature is observed when the sample is cooled down (Fig. 2b). The activation energy for the higher temperature region of exponential increase in the signal intensity (2.23 eV for 2% Cr-doped sample), determined from the corresponding Arrhenius plot, indicates that the desorption of the constitutional potassium (located in the interlayer spaces of β-ferrite) takes place. On the other hand, the low temperature maximum is associated with a minute amount of loosely bounded potassium which segregated at the basal planes of the ferrite surface during the synthesis. Since after the second heating run the segregated potassium is completely depleted (Fig. 2b), this form of potassium is irrelevant for the overall potassium loss from the working catalyst.

For all the investigated samples the atomic flux overwhelmed the ionic one, which means that the main channel of potassium loss from the catalyst is due to atoms (equivalent to potassium volatilization process). The statistical probability of the ratio of ionic and neutral fluxes (j_+/j_0) from the surface is given by the Saha–Langmuir equation [20]:

$$\frac{j_+}{j_0} = \frac{g_+}{g_0} \exp\left[-\frac{e(V-\Phi)}{k_B T}\right] \quad (1)$$

where, g_+/g_0 is the ratio of the statistical weights of the ionic and atomic states (for potassium equal to 1/2) and e, V, Φ, k_B and T denote elementary charge, ionization potential of desorbing atom (for potassium 4.3 eV), work function of the surface, Boltzmann constant and temperature, respectively. As implied by Eq. (1) the extent of surface ionization of potassium is strongly associated with a work function of the samples. Indeed, the flux of the atomic potassium desorption from the β-ferrite samples was found to correlate linearly with the work function changes induced by potassium depletion and determined from the contact potential measurements (Fig. 3). The intentional modification of the work function can also be effected by appropriate doping. In Fig. 4 the effect of several additives (such as Mn, Cr, Mg, Al, and Ce) typically used in the real iron-oxide catalyst on the potassium stabilization expressed as flux intensity (S_K) and activation energy of K desorption $E_{des}(K)$ is plotted versus work function (Φ) of doped β-ferrite. It can be inferred that among the investigated dopants, cerium exhibit the highest shift in work function and corresponding stabilization of potassium (the highest $E_{des}(K)$ and the lowest S_K). Taking into account that the cerium, being not incorporated into the ferrite structure, is located in the form of nanocrystallites segregated on the basal planes (Fig. 1), its influence on the potassium desorption should be of a remote electronic nature. Consequently, the increase in work function, following the Eq. (1), strongly favors the less volatile cationic state of potassium at the surface.

In the case of chromium the origin of its beneficial effect is different as it can be inferred from the observed changes in the work function of the undoped and Cr-doped β-ferrite in time, shown in Fig. 5. They can be associated with the potassium diffusion in the interlayer space towards the external surface. The determined rate constant of $3.1 \pm 0.5 \times 10^{-4}\,s^{-1}$ and $2.1 \pm 0.6 \times 10^{-6}\,s^{-1}$ for undoped and Cr-doped β-ferrite, respectively, reveals a clear hindrance of potassium diffusion invoked by Cr-doping. In contrast to chromium, in the case of the Ce-doped samples this effect was found to be practically buried within the experimental error ($1.6 \pm 0.8 \times 10^{-4}\,s^{-1}$) in agreement with the electronic origin of its stabilization, as discussed above.

Two types of proposed potassium stabilization effects in β-ferrite are summarized in Fig. 6. The extra-pillars potassium-blocking model developed in [21] provides suitable conceptual background for description of the observed significant stabilization of β-ferrite by chromium doping. As discussed therein Cr^{3+} ions, due to their high octahedral crystal field stabilization energy, substitute for Fe^{3+} ions in Fe1 positions. The latter, in turn, are displaced to the interlayer space (Fe3), forming new extra-pillars Fe_T–O–Fe_T, on filing tetrahedral sites (Fig. 6). Because potassium transport to the surface is controlled by the diffusion through the interlayer space (gallery), the steric hindrance induced by the generated extra-pillars leads to blocking the K^+ diffusion pathway. In the case of cerium a detailed physical picture is less clear at this stage of investigations. Nonetheless, it can be substantiated in terms of a tangible correlation between work function and extinguishing of the atomic potassium flux (Fig. 3). Taking into account the location of cerium dopant at the basal hexagonal planes, it can be proposed that K^+ ions released from the bulk diffuse to the external surface, and are stabilized due to enhanced work function in the vicinity of the ceria crystallites.

4. Conclusions

Basing on potassium thermal desorption experiments and work function measurements, two main mechanisms of the potassium stabilization in β-ferrite can be exploited depending on the dopant location. Incorporation of Cr into the structure of β-ferrite slows down potassium diffusion from the bulk towards the external surface, whereas the additives (such as CeO_2) located at the basal planes via work function increase favor the surface ionization and thus decrease the probability of potassium atoms to leave the β-ferrite phase—the active component of iron-oxide catalyst.

Acknowledgment

This work was sponsored by the Polish Ministry of Science and Higher Education under Research Project N N205 2946 33.

References

[1] D. Resasco, in: I.T. Horvath (Ed.), Encyclopedia of Catalysis, vol. 3, Wiley, Hoboken, 2003, p. 76.
[2] K. Kochloefl, M. Muhler, in: G. Ertl, H. Knözinger, F. Schuth, J. Weitkamp (Eds.), Handbook of Heterogeneous Catalysis, vol. 7, Wiley-VCH, Weinheim, 2008, p. 3229.
[3] M. Muhler, J. Schütze, M. Wesemann, T. Rayment, A. Dent, R. Schlögl, G. Ertl, J. Catal. 126 (1990) 339.
[4] A. Trovarelli, C. De Leitenburg, M. Loaro, G. Dolcetti, Catal. Today 50 (1999) 353.
[5] T. Hirano, Appl. Catal. 26 (1986) 65;
T. Hirano, Appl. Catal. 28 (1986) 119.
[6] N. Dulamita, A. Maicaneanu, D.C. Sayle, M. Stanca, R. Cracium, M. Olea, C. Afloroaei, A. Fodor, Appl. Catal. A: Gen. 287 (2005) 9.
[7] T. Hirano, Bull. Chem. Soc. Japan 59 (1986) 2672.
[8] A. Miyakoshi, M. Ueno, M. Ichikawa, Appl. Catal. A: Gen. 216 (2001) 137;
A. Miyakoshi, M. Ueno, M. Ichikawa, Appl. Catal. A: Gen. 219 (2001) 249.
[9] F. Cavani, F. Trifiro, Appl. Catal. A: Gen. 133 (1995) 219.
[10] S.-J. Liao, T. Chen, C.-X. Miao, W.-M. Yang, Z.-K. Xie, Q.-L. Chen, Catal. Commun. 9 (2008) 1817.
[11] H.E.L. Bomfim, A. Conceição Oliveira, M. do Carmo Rangel, React. Kinet. Catal. Lett. 80 (2003) 359.
[12] G.R. Meima, P.G. Menon, Appl. Catal. A: Gen. 212 (2001) 239.
[13] L. Holmlid, P.G. Menon, Appl. Catal. 212 (2001) 247.
[14] M. Muhler, R. Schlögl, G. Ertl, J. Catal. 138 (1992) 413.
[15] A. Kotarba, I. Kruk, Z. Sojka, J. Catal. 211 (2002) 265.
[16] A. Kotarba, W. Rożek, I. Serafin, Z. Sojka, J. Catal. 247 (2007) 238.
[17] S. Ito, M. Washio, I. Makino, N. Koura, K. Akashi, Solid State Ionics 86 (1996) 1005.
[18] L. Holmlid, J. Phys Chem. A 102 (1998) 10636.
[19] S. Ito, H. Kurosawa, K. Akashi, Y. Michiue, M. Watanabe, Solid State Ionics 86 (1996) 745.
[20] E.Y. Zandberg, Tech. Phys. 9 (1995) 865.
[21] I. Serafin, A. Kotarba, M. Grzywa, Z. Sojka, H. Bińczycka, P. Kuśtrowski, J. Catal. 239 (2006) 137.